United Atom Force Field for Phospholipid Membranes: Constant Pressure Molecular Dynamics Simulation of Dipalmitoylphosphatidicholine/ Water System

ALEXANDER M. SMONDYREV, MAX L. BERKOWITZ

Department of Chemistry, University of North Carolina at Chapel Hill, Chapel Hill, North Carolina 27599

Received 24 July 1998; accepted 12 November 1998

ABSTRACT: We refined the united atom field for the simulations of phospholipid membranes. To validate this potential we performed 1000-ps constant pressure simulation of a dipalmitoylphosphatidicholine (DPPC) bilayer at $T = 50°$ C. The average area per head group (61.6 $\pm$ 0.6) Å^2 obtained in our simulation agrees well with the measured one of (62.9 $\pm$ 1.3) Å^2. The calculated S_{CD} order parameters for the Sn-2 hydrocarbon tail also display a good agreement with the experiment. The conformations of head groups in our simulations of the liquid crystal phase are different than the ones observed in the crystal structure. © 1999 John Wiley & Sons, Inc. J Comput Chem 20, 531–545, 1999

Keywords: phospholipid membranes; force field; united atom; molecular dynamics; DPPC bilayer

Correspondence to: M. L. Berkowitz; e-mail: maxb@net.chem.unc.edu

Contract/grant sponsor: National Science Foundation; contract/grant number: MCB9604585

CCC 0192-8651 / 99 / 050531-15

Introduction

Recently there was a lot of activity in performing molecular dynamics computer simulations on model biomembranes containing molecules such as dipalmitoylphosphatidylcholine (DPPC) and dilauroylphosphatidylethanolamine (DLPE).[1] A certain number of issues needed to be resolved before a meaningful comparison between experiment and simulation could be performed. Thus, for example, one had to understand what is the appropriate choice of an ensemble in the simulation (constant pressure[2–5] vs. constant volume[6–8] or constant surface tension[9,10]). For the lamellar system that often exists in the experiment, periodic boundary conditions are the best in mimicking the experiment. Therefore, one needed to develop and refine methods to speed up the calculation of long range forces using the Ewald summation technique.[11] While the issues related to the methodology of computer simulations play an important role in the comparison between theory and experiment, the choice of the force field plays a crucial role in the quality of the simulation.

It was shown that simulations that use CHARMM[12] all atom force fields can reproduce (and confirm) the experimental data related to the geometry, order, and short time dynamics in these membranes.[2,13] At the same time one would like to perform simulations using the united atom force field, because this model requires much less computational intensity. This feature makes it especially attractive for use in problems concerned with modeling the behavior of very large systems such as proteins in lipid membranes.[14] Force fields for united atom models are included in such packages as AMBER[15] and GROMOS,[16] but these were originally designed to describe proteins and nucleic acids. Thus, their application to membrane modeling is not straightforward.

In this article we report the refinement of the united atom force field that is based on the AMBER force field and that can be used for simulation of model biomembranes. In the following section we discuss the strategy of the parameter development for this force field. We tested the developed force field in the constant pressure simulation of the liquid crystal phase of the DPPC membrane. We present the methodology used in our simulations. The results of this simulation and comparison with experiments are presented. We conclude with a brief discussion.

United Atom Force Field Parametrization for DPPC

Our parameter development followed the procedure outlined by Schlenkrich et al.[17] We focused our efforts on obtaining an accurate set of torsional parameters, corresponding to a set of atomic partial charges obtained for DPPC and DMPC molecules by Chiu et al.[9] Wherever possible, we adopted bond and angle parameters from the AMBER force field. Torsional parameters were fitted to reproduce geometry and energy profiles obtained from *ab initio* calculations of model compounds. To find the torsional parameters we divided the phospholipid molecule into five groups in the same way as Chiu et al.[9] (see Fig. 1). Head group 1 was subdivided into two subgroups: choline and phosphate. To obtain the torsional parameters for the head group we considered three model compounds (ethyltrimethylammonium, choline, and dimethyl phosphate). Torsional parameters for the two ester groups (2 and 3) were obtained by modeling methyl acetate, ethyl acetate, and methyl propionate. These were also considered by Schlenkrich et al.[17] In the calculations

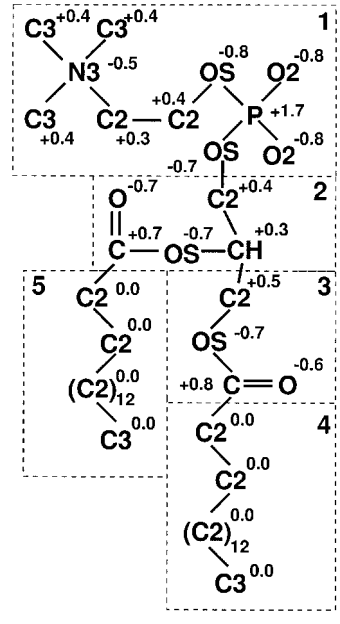

FIGURE 1. Atomic charges and AMBER atom types of the DPPC molecule.

with model compounds the charges on atoms were the same as in Schlenkrich et al.[17] with the united atom partial charges obtained by summing hydrogen charges into heavy atoms. These charges differ slightly from those used by Chiu et al.[9] The difference is due to the fact that the charges of Schlenkrich et al.[17] were calculated for fragments, while the charges from Chiu et al.[9] were obtained from calculations done on the whole molecule. The difference in two sets of charges is mostly due to the interaction between nitrogen and phosphorus groups, which is strong and therefore should influence the charge distribution. Nevertheless, we should mention here that the difference between the two sets of charges is smaller than the charge variation due to different molecular conformations. (Partial charges are dependent on molecular conformations. For example, see the charges calculated by Pasenkiewicz–Gierula et al.[18] for DMPC in the crystal and liquid crystalline phase.)

We calculated torsional energy profiles of model compounds, so that the total energy fitted the *ab initio* energy profiles obtained from Gaussian calculations.[17] During the optimization of torsional parameters, the torsional angle of interest was set to a specified value and all other degrees of freedom were allowed to relax. Energy minimization was performed using the SANDER module of AMBER version 5.0. The electrostatic calculations were done with a dielectric constant $\varepsilon = 1$ and a 10-Å cutoff. The 1–4 van der Waals interactions were divided by 8.0 and the electrostatic by 2.0. The OPLS parameters[19] used for the van der Waals interactions are given in Table I.

We calculated the geometries of different conformations of model compounds and compared them with those obtained from *ab initio* calculations and calculations with the CHARMM force field. Because we adopted the angle bend parameters from standard force fields (either CHARMM or AMBER), we verified that equilibrium angles were in agreement with the *ab initio* calculations and in agreement with the experiment. Minimum energy and transition state configurations were obtained using module NMODE in the AMBER simulation package.

We used the Ryckaert–Bellemans potential[20] to describe the hydrocarbon torsional energy of the hydrocarbon chains (groups 4 and 5).

Below we describe the derivation of torsional parameters that were used in the simulations. The full set of force field parameters used for the DPPC/water system is listed in Table I.

HEAD GROUP

Ethyltrimethylammonium

The atom numbering and partial charges used to model ethyltrimethylammonium are shown in Figure 2(a). The trans orientation of the C4—N—C1—C5 dihedral corresponds to a minimum energy configuration and the cis orientation corresponds to a transition state. These two states are separated by a 5.5 kcal/mol barrier above the trans minimum. Torsional parameters were fitted to reproduce this potential barrier. The values of internal coordinates for trans and cis states were compared with those obtained from *ab initio* calculations and calculations with the CHARMM force field developed by Schlenkrich et al.[17] (see Table II). As one can see from Table II, the geometries obtained using united atom parametrization are in a good agreement with the model where hydrogens were included explicitly. The value of the optimized torsional parameter for the C3—N3—C2—C2 (see Fig. 1) dihedral $V_3/2 =$ 0.6 kcal/mol is slightly larger than the one in the AMBER force field of $V_3/2 = 0.47$ kcal/mol.[15]

Choline

Torsional parameters for dihedral N—C1—C5—O were obtained by modeling choline itself. Atom numbering and partial charges used in modeling choline are shown in Figure 2(b). *Ab initio* calculations[17] found two stable states for the dihedral angle $\tau_{N-C1-C5-O} = 56°$ (the energy minimum state, which we call gauche) and $\tau_{N-C1-C5-O} = 180°$ (trans state). The transition state between the two gauche structures ($\tau_{N-C1-C5-O} = 0°$) is called cis, and the state between the trans and gauche conformers ($\tau_{N-C1-C5-O} = 130.5°$) is called TS. The energy of the trans structure is about 4.3 kcal/mol higher than the minimum [the average of the values obtained using 6–31G(d) and 6–31G(d, p) sets], and the barriers are 5.2 kcal/mol for the cis state and 6.2 kcal/mol for the TS state.[17] The potential energy diagram of these states is depicted in Figure 3. The gauche conformation is favorable due to the interaction between oxygen and the CH_3 group. This interaction tries to minimize the distance between the two groups. The behavior of the N—C1—C5—O dihedral is rather important in determining the structural properties of the lipid bilayer. Robinson et al.[6] reported that 82% of these dihedrals were trans in their simulation of lipid bilay-

TABLE I.
United Atom Force Field Parameters.

Bond Parameters

Bond	r_{eq} (Å)	Bond	r_{eq} (Å)	Bond	r_{eq} (Å)	Bond	r_{eq} (Å)
N3—C3	1.510	C2—C3	1.526	C2—C	1.522	P—OS	1.610
N3—C2	1.510	C2—CH	1.526	C—O	1.220	P—O2	1.480
C2—C2	1.526	C2—OS	1.425	C—OS	1.334		

Angle Parameters

Angle	K_θ [kcal / (mol rad^2)]	θ_0 (°)	Angle	K_θ [kcal / mol rad^2)]	θ_0 (°)
C2—N3—C3	60.0	109.5	C2—CH—C2	63.0	111.5
C3—N3—C3	60.0	109.5	C2—OS—C	40.0	109.5
N3—C2—C2	80.0	111.2	CH—OS—C	40.0	109.5
C2—C2—OS	80.0	109.5	OS—C—O	90.0	125.9
CH—C2—OS	80.0	109.5	OS—C—C2	55.0	109.0
C2—CH—OS	80.0	109.5	O—C—C2	70.0	125.0
C2—OS—P	100.0	120.5	C—C2—C2	63.0	112.4
OS—P—O2	100.0	108.2	C2—C2—C2	63.0	112.4
OS—P—OS	45.0	102.6	C2—C2—C3	63.0	112.4
O2—P—O2	140.0	119.9			

Torsional Parameters

Torsion	$V_n/2$ (kcal / mol)	γ (°)	n[a]	Torsion	$V_n/2$ (kcal / mol)	γ (°)	n[a]
C3—N3—C2—C2	0.6	0	3	C2—CH—OS—C	0.4	0	−3
N3—C2—C2—OS	1.9	0	−3	C2—CH—OS—C	1.5	180	2
N3—C2—C2—OS	−1.0	180	1	CH—C2—OS—C	0.4	0	−3
C2—C2—OS—P	1.45	0	3	CH—C2—OS—C	1.5	180	2
CH—C2—OS—P	1.45	0	3	C2—OS—C—O	5.6	180	−2
C2—OS—P—O2	0.25	0	3	C2—OS—C—O	0.7	0	1
C2—OS—P—OS	0.25	0	−3	CH—OS—C—O	5.6	180	−2
C2—OS—P—OS	1.1	0	2	CH—OS—C—O	0.7	0	1
OS—C2—CH—OS	1.0	0	−3	CH—OS—C—C2	1.0	180	2
OS—C2—CH—OS	0.5	0	2	C2—OS—C—2	1.0	180	2
OS—C2—CH—C2	1.0	0	3	OS—C—C2—C2	0.3	0	−3
C2—C2—C—O	0.0	0	3	OS—C—C2—C2	0.8	180	2

Van der Waals Parameters

Atom Type	σ (Å)	ε (kcal / mol)		Atom Type	σ (Å)	ε (kcal / mol)	
C2	3.905	0.118	OPLS[19]	N3	3.250	0.170	OPLS
C3	3.905	0.175	OPLS	P	3.740	0.200	OPLS
CH	3.850	0.080	OPLS	OW	3.150	0.152	TIP3P water[27]
C	3.750	0.105	OPLS	HW	1.000	0.000	TIP3P water
OS	3.000	0.170	OPLS	C2[b]	3.960	0.091	Berger et al.[5]
O2	2.960	0.210	OPLS	C3[b]	3.960	0.136	Berger et al.
O	2.960	0.210	OPLS				

[a]The periodicity of the torsion; negative value indicates that there is more than one component in the torsional potential.
[b]For atoms in the hydrocarbon tails.

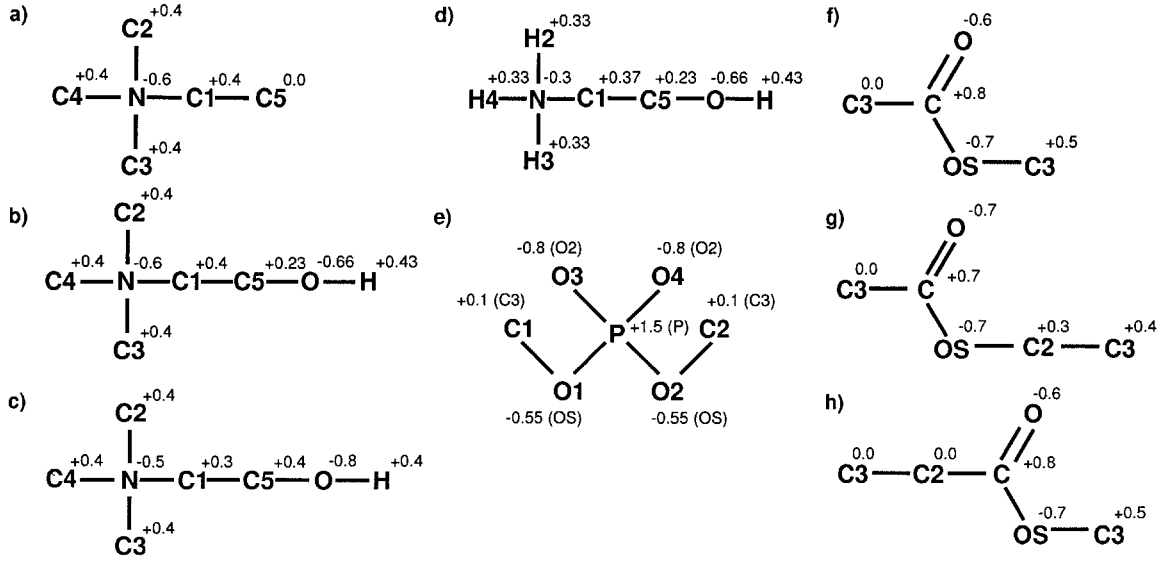

FIGURE 2. Atom numbering, partial charges, and atom types of the model compounds: (a) ethyltrimethylammonium, (b) choline, (c) choline with the set of atomic charges from the DPPC molecule, (d) ethanolamine, (e) dimethyl phosphate, (f) methyl acetate, (g) ethyl acetate, and (h) methylproprionate.

ers in the liquid crystal state. They attributed this to a deficiency in a force field potential that they used. Shinoda et al.[3] observed a similar effect in their constant pressure simulation. It is possible that the low area per head group ($A = 54$ Å^2) that they observed is due to the incorrect behavior of the N—C1—C5—O dihedral. For the trans conformation of the N—C1—C5—O dihedral the head group is extended along the direction perpendicular to the membrane surface. This is observed in the crystal and gel phases of DPPC, where the angle between the P−N vector and the plane of the membrane is large. In the crystal and gel phases the area per head group is much lower than in the liquid crystal phase. Because careful parametrization of this particular dihedral is important if one wants to reproduce conformational properties of the membrane lipids, we pay special attention to it. A combination of onefold and threefold torsion parameters was used to reproduce the *ab initio* energies of the four conformations described above. Parameters obtained from the best fit are listed in Table I.

The optimized value of the N—C1—C5—O dihedral angle from our calculations is 59.2°, which is in good agreement with the values obtained from the *ab initio* calculations (56.0°) and CHARMM (59.9°). Because the charges for the choline group are slightly different in the DPPC compared to a choline fragment, we studied the effects due to the charge variations. The model of the choline fragment that differs from the previous

TABLE II.
Geometries and Optimized Structures of Ethyltrimethylammonium.

	Trans			Cis		
	This Work	*Ab Initio*	CHARMM	This Work	*Ab Initio*	CHARMM
C1—N—C4	108.0	107.8	110.4	115.9	113.8	111.4
C1—N—C2(3)	111.5	111.1	110.2	108.2	109.1	110.0
N—C1—C5	115.2	116.0	114.6	117.3	116.9	115.8
C5—C1—N—C2(3)	61.5	61.1	59.9	121.6	120.7	120.1

The angles are in degrees. The trans and cis states are defined through the C5—C1—N—C4 dihedral. Results obtained from *ab initio* and CHARMM force field calculations are taken from Schlenkrich et al.[17]

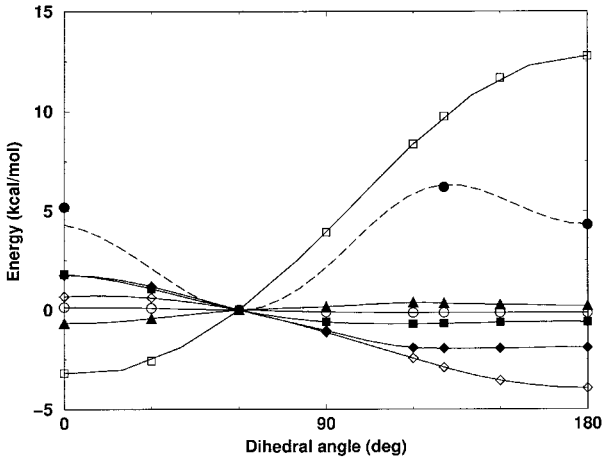

FIGURE 3. Energy profile as a function of the N—C1—C5—O dihedral angle in choline. (---) Total energy, *ab initio*, (□) electrostatic without 1–4 contribution, (◇) 1–4 electrostatic, (◆), VDW without 1–4 contribution, (▲) 1–4 VDW, (■) bond angle, and (○) bond stretch.

one only in the values of partial charges is shown in Figure 2(c). All charges except for the hydrogen (which is absent in DPPC) were taken as in DPPC. The charge on the hydrogen was chosen so that the total charge of the choline was 1.0 as in the model of Schlenkrich et al.[17] We used torsional parameters obtained from the model depicted in Figure 2(b). The geometries and the relative energies, calculated for the choline with DPPC charges are given in Table III. The geometries of choline calculated using four different methods are in a good agreement with each other; the variation of charges has a very minor effect on them. The relative energies of the conformations are more sensitive to the charge variations as one can see from Table III. There is a strong interaction between phosphate and nitrogen groups in DPPC, which tries to keep these two groups in close proximity. Table III shows that this result in the increase of the barrier between the gauche and trans states, which enhances the trend for the dihedral to be in a gauche state. Therefore, a substitution of charges in the choline fragment acts as an indirect test of how the environment (in our case the phosphate group) affects the behavior of the choline group in DPPC.

To perform further tests of the derived torsional parameters for the N—C1—C5—O dihedral we modeled ethanolamine. It has the same general structure as choline, but the CH_3 groups are replaced by hydrogens in the amine group. The model of ethanolamine with its partial charges is shown in Figure 2(d). Because nitrogen is of the same type (in the sense of AMBER's atom types), we used the same torsional parameters for N—C1—C5—O as in choline rather than defining a new set. This procedure is suggested in AMBER[15] for developing new parameters when no specific parameters are available. Geometries for the four states are compared with *ab initio* and CHARMM results in Table III. The relative energies of the trans and gauche states from the *ab initio* and this work are also given in Table III.

Our predictions for the ethanolamine geometries are in a good agreement with the *ab initio* calculations. Although there is a difference in the relative energies of trans states obtained from the *ab initio* calculations and calculations using united atom parametrization, this should not affect the results of simulations at temperatures typical for lipid membranes, because the absolute value of the barrier is high relative to the temperature. Our results indicate that the suggested parametrization of the N—C1—C5—O dihedral angle may be applied to a relatively wide variety of partial charges and even to different compounds. At the same time caution should be exercised because the conformation of choline in the united atom model is sensitive to the particular treatment of electrostatic interactions. Thus, a test similar to the one done in this work is suggested when applying this parametrization to a different system or with a different set of charges.

Phosphate Group

To complete the parametrization of the head group we used dimethyl phosphate (DMP) [see Figure 2(e)] to find parameters for the phosphate group. We considered two sets of charges: one suggested by MacKerell et al.[21] for parametrization of nucleic acids and a second based on DPPC charges. To adopt DPPC charges for DMP we adjusted the charges of C3 atoms to obtain a total charge of -1.0. As we will show later, this did not change the geometries and relative energies of different states of DMP. Three conformations defined by the dihedral angles O1—P—O2—C2 and C1—O1—P—O2 [gauche–gauche (g, g), (gauche–trans (g, t) and trans–trans (t, t)] were considered for optimization. The value of gauche angle $\tau = 72°$ was obtained from the *ab initio* calculation.[21] For optimization we assumed that the general torsional parameters for X—OS—P—X are the same as in AMBER force field[22] (see Table I) and added a twofold torsional potential

TABLE III.
Geometries of Optimized Structures and Relative Energies (kcal / mol) of Choline and Ethanolamine.

		Cis	Gauche	TS	Trans
		Choline			
N—C—C	*Ab initio*	119.1	116.6	116.2	116.8
	CHARMM	121.4	119.1	117.7	117.6
	This work, fragment charge	119.6	116.6	114.6	115.0
	This work, DPPC charge	119.5	116.4	114.8	115.4
C—C—O	*Ab initio*	112.1	109.6	105.2	102.5
	CHARMM	115.4	111.6	104.7	104.4
	This work, fragment charge	114.3	111.2	108.3	108.6
	This work, DPPC charge	113.3	110.1	107.5	107.9
ΔE	*Ab initio*	5.2	0	6.2	4.3
	CHARMM	4.2	0	6.2	5.2
	This work, fragment charge	4.3	0	6.3	4.3
	This work, DPPC charge	3.4	0	8.9	7.6
		Ethanolamine			
N—C—C	*Ab initio*	109.6	107.9	111.3	111.0
	CHARMM	112.7	111.2	112.9	112.9
	This work, fragment charge	105.5	104.4	111.1	111.8
C—C—O	*Ab initio*	106.5	104.9	105.6	103.6
	CHARMM	112.6	110.0	108.6	107.7
	This work, fragment charge	105.7	103.7	108.1	108.4
ΔE	*Ab initio*		0		8.4
	This work, fragment charge		0		11.2

The angles are in degrees. *Ab initio* and CHARMM force field results are from Schlenkrich et al.[17]

for the C3—OS—P—OS dihedral. Parameters for this extra twofold term were then optimized. Relative energies of conformations from AMBER,[22] CHARMM,[21] and from our calculations with two sets of charges in the united atom model are listed in Table IV. The united atom parameterization of DMP suggested in this work is almost insensitive to the particular choice of atomic charges.

TABLE IV.
Relative Energies of DMP Conformations (kcal / mol).

	gg	*gt*	*tt*
AMBER	0	1.42	2.83
CHARMM	0	1.38	1.40
Ab initio	0	1.40	3.44
This work, fragment charge	0	1.40	3.10
This work, DPPC charge	0	1.50	3.20

We compare data obtained with the united atom force field with data from the AMBER force field,[22] CHARMM force field,[21] and *ab initio* calculations.[21]

ESTER

There are two ester groups in DPPC (indicated as 2 and 3 in Fig. 1) that link the head group with the hydrocarbon tails. We used the methyl acetate fragment [see Fig. 2(f)] to optimize torsional parameters of C3—OS—C—O dihedral and the ethyl acetate fragment [Fig. 2(g)] to obtain the torsional parameters for the C—OS—C2—C3. The charges for the models of methyl acetate and ethyl acetate were chosen as the ones used in groups 2 and 3 of the DPPC molecule. Because both groups are neutral; this adaptation was straightforward. We considered a model of methyl propionate [Fig. 2(h)] to obtain torsional parameters for the C3—C2—C—OS dihedral. As in the case of the phosphate and choline groups, we compared the results of the optimizations when two different sets of charges were used.[9,17] We found that the charge variation had a negligible effect on the conformational geometry and energetics of ester groups. For all model compounds considered in

this section we used improper dihedral potential to ensure the planarity of the ester groups. The angle parameters for the ester group that were not available in the standard AMBER force field were taken from force fields developed by Schlenkrich et al.[17] and Stouch et al.[23]

Methyl Acetate

There are only two dihedral angles in the model methyl acetate. Several parametrizations for C3—C—OS—C3 are available (AMBER,[15] CHARMM,[17] Stouch et al.,[23] and Tu et al.[24]), which quote similar values for $V_2/2$. Thus, it was only necessary to optimize torsional parameters for the C3—OS—C—O dihedral. From the *ab initio* calculations[17] we know that there are two stable conformers of methyl acetate. Conformation Z is defined by the dihedral angle $\tau_{O=C-OS-C3} = 0°$ and corresponds to a minimum of energy. The energy of conformer E is 9.2 kcal/mol (average from *ab initio* calculations[17]) higher than the minimum and is characterized by the angle $\tau_{O=C-OS-C3} = 180°$. The barrier between states E and Z is 13.2 kcal/mol [the average of the values obtained using 6−31G(d) and 6−31G(d, p) sets] and is located in the vicinity of $\tau_{O=C-OS-C3} = 90°$. We used a combination of onefold and twofold torsional parameters to fit the *ab initio* data (see Table I). Geometries for the states E and Z obtained from the united atom parametrization are compared with the data available from the experiment,[25] *ab initio* calculations, and CHARMM parametrization[17] in Table V.

Ethyl Acetate

To optimize C—OS—C2—C3 torsional parameters we used a model of ethyl acetate. Again the *ab initio* data were taken from Schlenkrich et al.[17] Four conformational states were used for optimization. The relative energies of these conformations are listed in Table VI and are compared with values obtained from the united atom parametrization of this work. We used a combination of onefold and twofold potentials for the C—OS—C2—C3 dihedral. Our optimization attempted to fit primarily the relative energies of trans, gauche, and TS configurations. The relative energy of the cis conformation in our calculation was lower than the *ab initio* value but still high enough to represent the barrier between two symmetric gauche minima.

Methyl Propionate

The model of methyl propionate [Fig. 2(h)] was used to obtain torsional parameters for dihedral OS—C—C2—C3. There are two dihedrals for which we did not find suitable parameters in the AMBER force field. In addition to the one mentioned above, we need to have parameters for the O=C—C2—C3 torsional angle. To simplify the task we used the fact that the ester group is planar. Because of that, two dihedral angles of interest are not independent. In fact, the knowledge of one angle determines the second. So, we can assume that torsional parameters of the O=C—C2—C3 dihedral are zeros and optimize only parameters for the first dihedral. The procedure is the same as in ethyl acetate, except that in this case we used a combination of a twofold and a threefold poten-

TABLE VI.
Energies (kcal / mol) of Ethyl Acetate and Methyl Propionate Conformations.

	Ethyl Acetate		Methyl Proprionate	
	Ab Initio	This work	*Ab Initio*	This work
Gauche	0	0	0.96	0.8
Trans	−0.5	−0.5	0	0
TS	0.9	0.9	1.22	1.3
Cis	7.3	5.1	1.3	1.3

TABLE V.
Geometries of Optimized Structures of Methyl Acetate.

		Ab Initio		CHARMM		This work	
	Exp Z	E	Z	E	Z	E	Z
C3—C—OS	109.0	118.1	111.4	114.0	109.6	116.1	108.7
OS—C=O	125.9	119.3	123.4	124.1	125.9	122.6	126.6
C—OS—C3	114.8	122.8	116.9	121.6	114.3	123.3	112.0

The angles are in degrees.

tials (see Table I). In Table VI the relative energies of four conformations are given for the united atom parametrization and *ab initio* calculations for the *Z* conformer of methyl propionate.

HYDROCARBON TAILS AND LINKS BETWEEN GROUPS

For the hydrocarbon chains we used Ryckaert–Bellemans potential.[20] We used two different sets of Lennard–Jones parameters for the united CH_n groups in hydrocarbon chains (see Table I). For one set we used OPLS parameters[19] and for the other we used parameters obtained from the pentadecane and DPPC simulations of Berger et al.[5] The latter set of parameters was used in all our simulations unless otherwise noted. Conservation of the chirality of the CH carbon (see Fig. 1) was achieved by applying a harmonic improper dihedral potential $V(\phi) = V_0(\phi - \phi_0)^2$, where ϕ is the dihedral angle, potential strength $V_0 = 50$ kcal/(mol radian^2), and equilibrium angle $\phi_0 = 120°$. The value of the equilibrium angle was taken from the energy minimization data for DMPC.[26] It is also consistent with the AMBER united atom parametrization[15] (X—CH—C2—X improper dihedral). Finally, to obtain a complete set of torsional parameters we needed to choose parameters for dihedrals that link different groups considered above. These parameters were taken from the AMBER force field. Parameters for the OS—C2—CH—C2 and OS—C2—CH—OS were originally derived from sugar model compounds. The choice of parameters for P—OS—C2—C2 torsion, which links phosphate and amine groups, is not obvious. Different groups quoted a variety of values used for this dihedral. Our choice was based on the AMBER force field, and there is no guarantee that it is optimal for the DPPC simulations.

Methods

To test the force field we performed molecular dynamics simulation on a DPPC bilayer in water. Our system consisted of 64 DPPC molecules and 1312 water molecules, which corresponds to 20.5 waters per lipid. The water model employed in our simulations was TIP3P.[27] The initial configuration was prepared using a method outlined by Tu et al.[2] We started with coordinates of two distinct conformations of DMPC in a crystal asymmetric unit determined by Vanderkooi[26] and added two carbon atoms to each tail. The coordinates of the center of mass were adjusted so that the area per head group was 62 Å^2 and a second molecule was shifted up so that phosphorus atoms of both molecules were on the same level. This was done to disrupt the crystal structure. After adjusting the coordinates the asymmetric unit was used as a building block to create a monolayer that consisted of 32 lipid molecules. This monolayer was equilibrated for 20 ps during which the phosphorus atoms were fixed. The lipid bilayer was created by applying the $P2_1$ symmetry group to the equilibrated monolayer and adjusting the distance between the phosphorus atoms of two halves of the bilayer to 38 Å. This bilayer was equilibrated for another 20 ps with fixed phosphorus atoms. At this stage we added 1312 water molecules to the system and gradually decreased the *z* dimension of the simulation cell to 60 Å. (This value was chosen by assuming that the volume per lipid molecule is 1.23 nm^3 and the volume per water molecule is 0.03 nm^3.) At each interlamellar distance the system was equilibrated for 2 ps, again keeping the phosphorus atoms fixed. After adding water and adjusting the dimensions of the simulation cell, we performed a 50-ps simulation with free phosphorus atoms. To ensure that the hydrocarbon tails were disordered, we increased the temperature to 423 K and then reduced it in a series of 20-ps simulations (T = 393, 363, 343, 333, and 323 K). Finally, we equilibrated the system at T = 323 K for 100 ps.

After equilibrating the system at constant volume, we performed a 1000-ps simulation at constant pressure (P = 0 atm) and temperature (T = 323 K) with periodic boundary conditions. We kept the angles of the simulation cell fixed and varied the dimensions of the cell using a Hoover barostat. The thermostat and barostat relaxation times were 0.2 and 0.5 ps, respectively. All bond lengths were held fixed using the SHAKE algorithm with a tolerance of 10^{-4}, allowing us to use the time step of 0.002 ps. The Ewals summation technique was used to calculate electrostatic contributions with a tolerance of 10^{-4}. The real space part of the Ewald sum and van der Waals interactions were cut off at 10 Å. Calculations were performed on a Cray-T3E at the North Carolina Supercomputer Center and a Cray-T3E at the San Diego Supercomputer Center using the DL–POLY simulation package version 2.8 developed in the Daresbury Laboratory in England.[28] A picosecond of simulation required approximately 15 min

of CPU time using eight processors running at 450 MHz.

Results

BILAYER GEOMETRY

One of the important parameters that describes the geometric arrangement of the bilayer is its area per head group. In Figure 4 we show the time evolution of the area per head group during the 1000-ps simualtion. The average area per head group is 61.6 ± 0.6 Å^2, which is in a good agreement with the experimental value[29] of 62.9 ± 1.3 Å^2 and with the result of the constant pressure simulation of Tu et al.[2] (61.8 Å^2). We also display the time dependence of the lamellar spacing in Figure 4. The averaged value of this spacing in our simulation is 59 ± 1 Å. The volume per lipid was calculated from the equation

$$V_{\text{tot}} = N_{\text{L}} \times V_{\text{L}} + N_{\text{W}} \times V_{\text{W}}. \qquad (1)$$

We obtained the average volume per lipid of V_{L} = 1.20 ± 0.01 nm^3 (the experimental value[30] is 1.23 nm^3) when using the above equation with the volume per water molecule of V_{W} = 30 Å^3. Our bilayer was stable throughout the simulation and acted as an incompressible fluid.

To see how modifications of parameters in the hydrocarbon tails affect the area per head group, we performed another simulation. In this simulation we used the OPLS set of Lennard–Jones parameters for the united CH_n groups in the hydrocarbon chains. The run started from the same initial configuration as in the simulation described above and lasted for 1300 ps. The area per head group as a function of time is shown on Figure 5. We can see that the bilayer is stable, but the average area per head group is 60.1 ± 0.8 Å^2. The average volume per lipid is also lower: V_{L} = 1.15 ± 0.01 nm^3. This confirms the observations made by Berger et al.[5] that the choice of parameters for hydrocarbon chains can influence the area per head group.

DENSITY PROFILES

We computed distances from the bilayer center to different carbon atoms in the lipid molecules and compared them with the results obtained in neutron diffraction experiments.[31] It should be noted that the diffraction experiments were performed at a lower hydration level (n_{w} = 13.6). For carbon atoms in the tails no distinction was made for atoms belonging to different chains. Shinoda et al.[3] observed that the Sn-2 chain is shifted up by approximately one carbon–carbon bond length. Because of this the error in the measurements

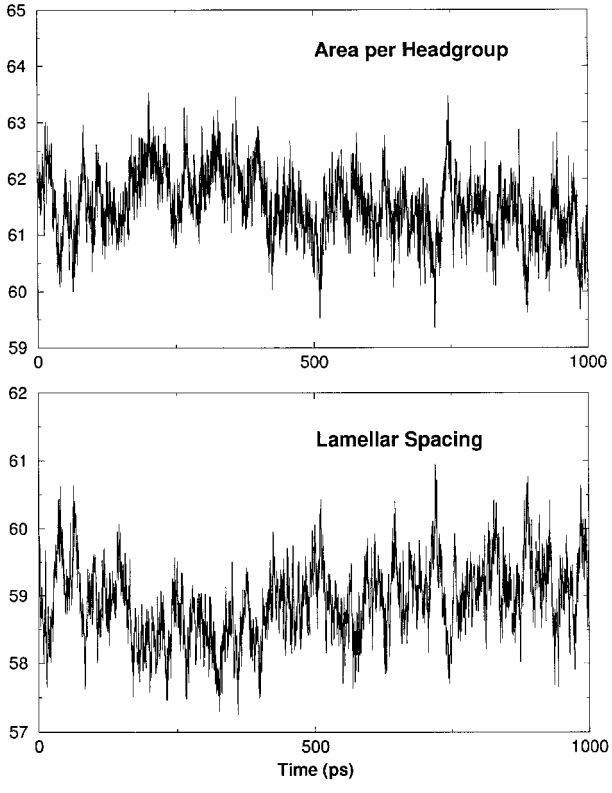

FIGURE 4. Time evolution of the area per head group in (Å^2) and lamellar spacing (Å).

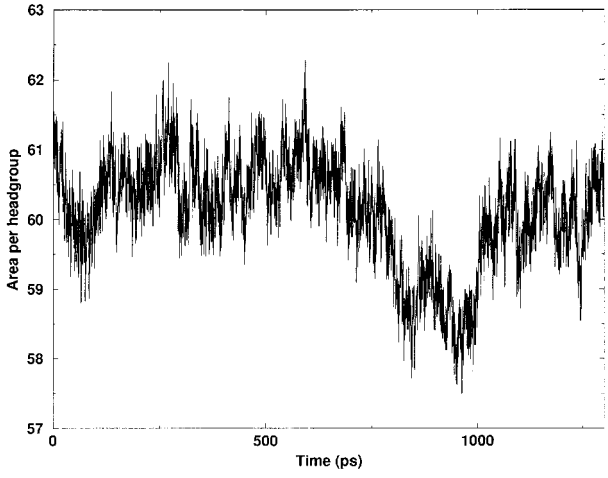

FIGURE 5. Time evolution of the area per head group (Å) in a constant pressure simulation for a model with OPLS tails.

increased and some discrepancies were observed. Nagle et al.[29] noted that the distance between C4 and C5 and between C14 and C15 is larger than the carbon–carbon bond length. In Table VII we compare results obtained in the liquid crystal simulation with the diffraction data. For the head group ammonium methyl carbon atoms C_γ we calculated the average distance between the center of the bilayer and all three atoms in the ammonium group. We also computed the electron density profile (see Fig. 6). The distance between the two peaks is approximately 36 Å, which is slightly lower than the distance between the phosphorus atoms (38 Å) found in our simulation. The experimentally determined peak to peak distance in the electron density profile ranged from 36.4 to 39.6 Å and depended on how the density was calculated.

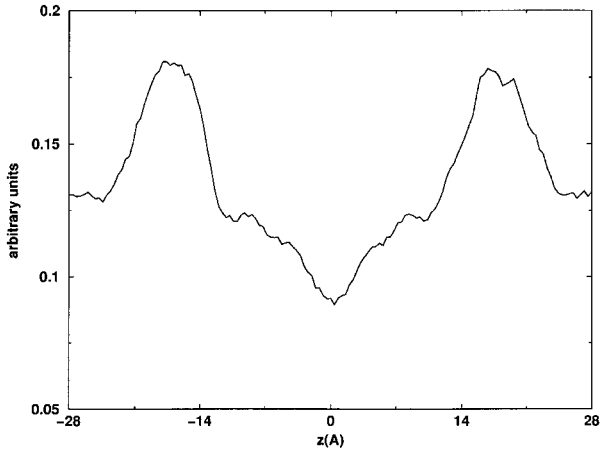

FIGURE 6. Electron density profile across the bilayer.

CHAIN ORDER PARAMETERS

The ordering in the tails of phospholipid molecules can be studied using the NMR technique by measuring the deuterium order parameter. This order parameter can also be calculated in the simulation from the expression[32]

$$-S_{\mathrm{CD}} = \frac{2}{3}S_{xx} + \frac{1}{3}S_{yy}, \qquad (2)$$

where $S_{ij} = \langle 1.5\cos\theta_i \cos\theta_j - 0.5\delta_{ij}\rangle$; θ_i is the angle between the ith molecular axis and the bilayer normal (axis Z). In Figure 7 we compare $|S_{\mathrm{CD}}|$ values for the Sn-2 chain from our simulation with the experimental results of Douliez et al.[33] The order parameter profile obtained in our simulation reproduces the experimental data of Douliez et al.[33] extremely well. The average value of the $|S_{\mathrm{CD}}|$ in the plateau region (from C4 to C8 carbon) is 0.216 in our simulation and 0.217 in the experiments of Douliez et al.[33] The average number of gauche conformers per chain was 3.5, including gauche defects at carbon C_2. This is in agreement with the IR data of Mendelsohn et al.[34] who reported a value of 3.9 for DPPC at $T = 50°$ C, the NMR measurements of Douliez et al.,[33] and the thermodynamic measurements of Nagle and Wilkinson[35] which both yielded a value of 3.8.

TABLE VII.
Distances from Bilayer Center (Å).

Carbon Atom	Simulation	Experiment
C_γ	19.53 ± 3.61	21.8 ± 0.6
C_α	19.47 ± 2.48	21.2 ± 1.0
C_β	19.39 ± 2.92	21.0 ± 1.0
CG-3	17.19 ± 2.03	17.4 ± 1.5
C4	11.75 ± 1.93	12.2 ± 1.5
C5	10.85 ± 1.92	10.5 ± 1.5
C9	7.14 ± 1.88	8.1 ± 1.0
C14	3.21 ± 1.74	3.6 ± 1.0
C15	2.06 ± 2.40	1.9 ± 1.0

BILAYER POTENTIAL

The total electrostatic potential across the bilayer is calculated from the expression

$$\psi(z) - \psi(0) = -\int_0^z dz' \int_0^{z'} \rho(z'')\, dz'', \qquad (3)$$

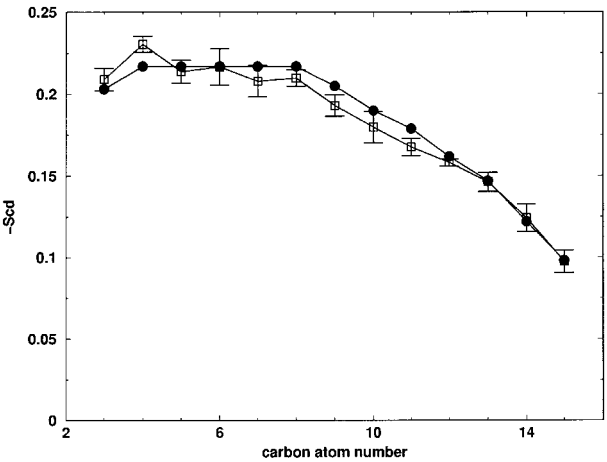

FIGURE 7. Hydrocarbon chain order parameter. (●) The experimental data, and (□) the present simulation. Error bars were obtained by dividing the run into five 200-ps blocks.

where $\rho(z)$ is the local excess charge density. The total potential and separate contributions due to the bilayer and water are shown in Figure 8. Although the experimental results for the electrostatic potential are not conclusive, Berger et al. suggested[5] that the overall shape of the potential is dependent on the fractional charges and can be used as a valuable tool to validate partial charges. In our simulation the potential (chosen to be zero inside the bilayer) initially increases at the interface and then drops to a value of -600 mV in the water. The shape of its profile is in a good agreement with the simulation results of Berger et al.[5] The potential difference between the water and bilayer interior of several hundred millivolts was also observed in the experiment.[36] As in the other simulations,[37] we observed that the sign of the potential is determined by the contribution of water into the total potential.

HEAD GROUP CONFORMATIONS

Because torsional parameters that are responsible for head group conformations were modified extensively, we studied the behavior of head groups in greater detail. There are different scenarios that describe this behavior. Because the liquid crystal phase is fluid, it is often difficult to make interpretations of the experimental results and computer simulations can provide valuable insight into the head group properties. One model suggests that there are free rotations in the head group, while another limiting model assumes that the structure of the head group is completely rigid. Different experimental studies produced results that supported both models. Several studies suggested that there is a possibility of an intermediate scenario in which some dihedral angles in the head group experience relatively free motion and some are fixed. Definitions of dihedral angles are shown in Figure 9, and their distributions with the fractions of trans conformations are shown in Figures 10 and 11. The conformation is defined as trans if the absolute value of the corresponding dihedral angle falls within the interval $120° < \tau < 240°$ and as gauche otherwise.

Figure 10 shows the distributions of torsional angles α_1–α_6. Akitsu[38] observed that the α_5 angle is predominantly gauche, which agrees with the results of our simulation and *ab initio* calculations for the choline fragment. The main peaks of the α_5 distribution correspond to $\pm 70°$, which is close to the α_5 value observed in the experiment performed on crystals[39] and also are in good agreement with the values obtained from the crystal

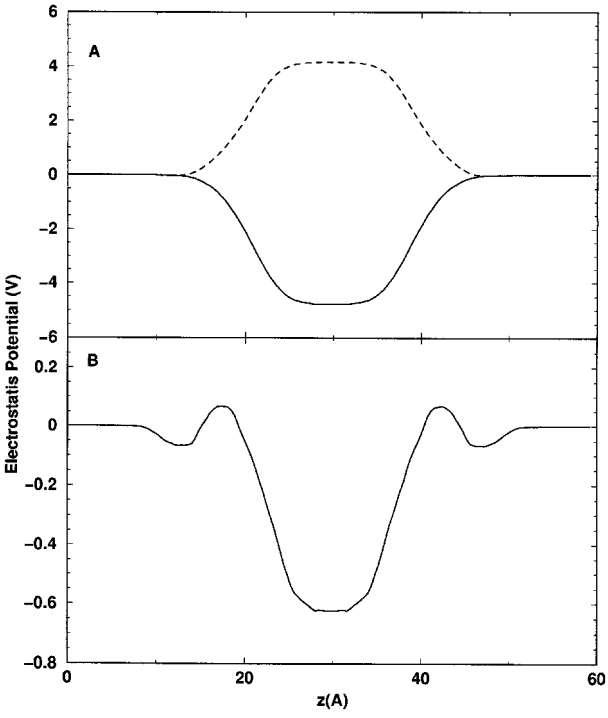

FIGURE 8. Electrostatic potential along the bilayer normal. (B) The total potential. (A) Separate contributions due to (—) water and (---) lipid are shown. Notice the difference in scale in the two parts.

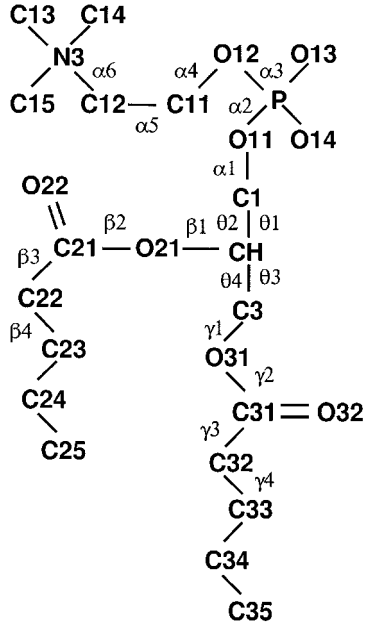

FIGURE 9. Definition of the dihedral angles adapted from Hauser et al.[43]

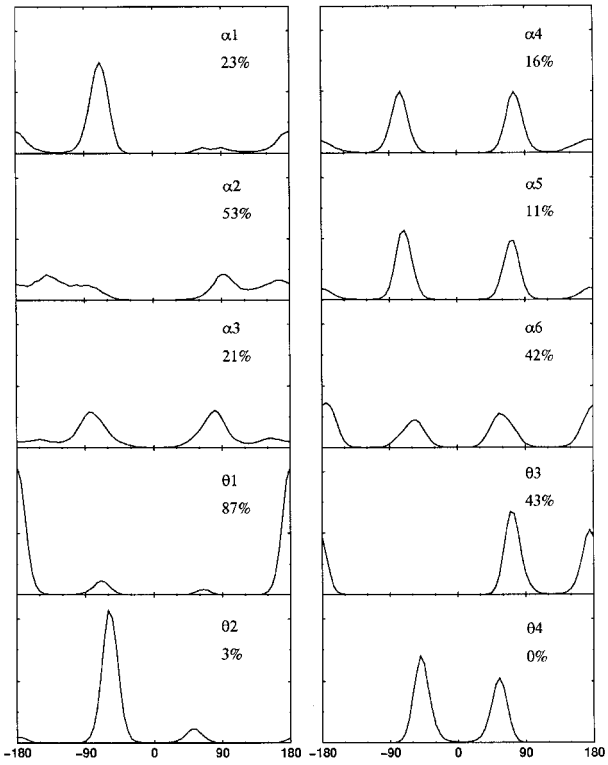

FIGURE 10. Distribution of dihedral angles $\alpha_1-\alpha_6$ and $\theta_1-\theta_4$.

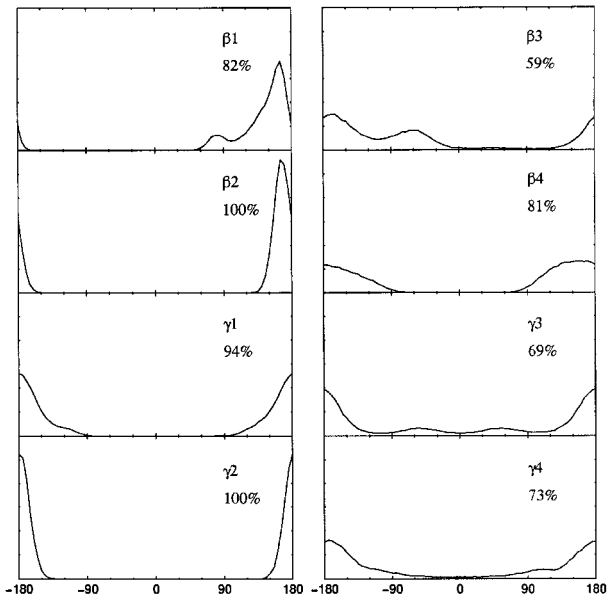

FIGURE 11. Distribution of dihedral angles $\beta_1-\beta_4$ and $\gamma_1-\gamma_4$.

energy minimization.[26] The next torsional angle α_4 is also predominantly gauche. In the crystal phase α_4 is trans. This difference might be due to the different areas per lipid in the crystal and liquid crystal phases. In the crystal phase the P–N vector makes a larger angle with the plane of the membrane to allow dense packing. In the liquid crystal phase the P–N vector lies almost parallel to the surface. Distribution of the angle between the P–N vector and the bilayer plane is shown in Figure 12. (The average value of this angle is 9°.) Note that in the gel phase simulation of Tu et al.[40] the average value for the P–N angle was 19°. This indicates that in the liquid crystal phase the head group conformation is more planar compared to the one in gel. The tendency of α_4 to adopt a gauche conformation creates a bend in the choline that brings phosphate and ammonium groups into a more planar conformation. The next two dihedral angles α_3 and α_2 define the conformation of the phosphate group. While the α_2 distribution is relatively broad, α_3 is mostly gauche. From *ab initio* calculations[21] we know that the minimum energy gauche angle is 72°, which agrees well with the observed values at gauche peaks. Because the lowest energy conformation of α_3, α_2 is gauche–gauche, it is natural that gauche conformations are dominant. The next lowest energy conformation is trans–gauche, which explains the increase in the number of trans conformations.

The conformation of the link between the phosphate group and glycerol is defined by α_1, which is predominantly gauche. On the basis of Raman spectroscopy studies, Bicknell–Brown et al.[41] concluded that the motional freedom of α_1 and α_4 dihedrals is greater than that of α_2 and α_3 dihedrals. For both α_1 and α_4 we observed that the fraction of trans conformations is low, while in

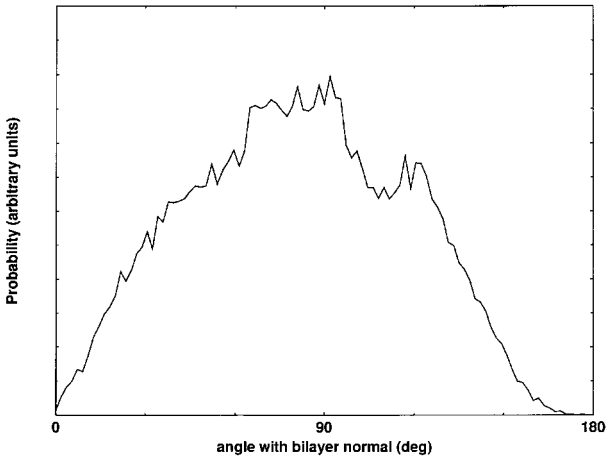

FIGURE 12. Distribution of the angle between the P–N vector and the bilayer normal.

the crystal phase these angles are trans. In case of α_1 this might be due to the interaction of phosphate and ester groups. Another possibility is that there is a problem with the torsional parameter for the rotation around the C2—OS bond. It should be mentioned that parameters for the P—OS—C2—C2(CH) torsion were not derived on the basis of *ab initio* calculations but were adopted from the standard AMBER force field file. (Values were taken from the general X—OS—C2—X dihedrals.) Although the values used to parameterize this dihedral are very close in the AMBER and GROMOS force fields, some other factors might influence the distribution of α_1. Although the procedure to determine torsional parameters for small model fragments is well established, there are no strict guidelines on how parametrization of links between different groups should be done.

Next we examine the distributions of θ angles of DPPC that are shown in Figure 10. In two molecules of crystal DPPC either θ_1 or θ_2 was in the trans state while the other was in the gauche state. In the gel phase simulation of Tu et al.[40] θ_1 was predominantly gauche, while θ_2 was mostly trans. We found that the torsional angle θ_1 is predominantly trans and θ_2 is predominantly gauche with a sharp peak at $-55°$. The distribution for the angle θ_3 obtained in our simulation deviates from the resolved crystal structures and gel phase simulation where θ_3 is exclusively trans. The distribution for θ_4 is peaked at $-50°$ and $+55°$. These values are close to the ones observed in crystals (63° and 51°).[39]

The distributions of torsional angles in two ester groups were similar to those observed in the crystal and gel phases. All four torsional angles in ester group 3 (see Fig. 1) $\gamma_1 - \gamma_4$ (Fig. 11) adopted predominantly trans conformations. The torsional angles in the other ester group (group 2, Fig. 1) exhibited a slightly different pattern (see Fig. 11). They had a slightly higher probability to be in the gauche state compared to corresponding angles in ester group 3. In the crystal phase the β_1 angle was 82° and 120° for DMPC-1 and DMPC-2 molecules, respectively. Using energy minimization Vanderkooi[26] found that in DMPC-2 this angle is 155°. In the liquid crystal phase we also observed that conformations of β_1 are predominantly trans. For β_2 we observed the same distribution as in the gel phase studies. The last two angles had a major effect on the conformation of the hydrocarbon chain Sn-2 because they defined how this chain was attached to the ester group. The range of average values of β_3, which were based on the crystal data of Pearson and Pasher[39] and the energy minimization of Vanderkooi,[26] was relatively wide. Tu et al.[40] found that the distribution of β_3 is also relatively wide (compared to other torsional angles in the ester groups) in the gel phase. In the liquid crystal phase β_3 exhibits a similar pattern. The probabilities of trans and gauche conformations are almost equal, and peaks are relatively wide. The distribution of β_4 shows that this conformation is predominantly trans in contrast to the findings for the crystal phase. In the gel phase the distribution of this angle was sharply peaked at around 180°.

Our data suggest that distributions of torsional angles in the DPPC head group do not have the same pattern as in the crystal phase. Although some conformational distributions are similar to the ones observed in the crystal phase, an increase in temperature and area per head group caused noticeable changes in the conformational structures of the DPPC molecules. We also found that the conformations of two ester groups were different, especially for the torsional angles defining the orientation of the initial segments of the hydrocarbon tails. The consequences of this effect will be studied in greater detail in future work.

Discussion

We extended the AMBER united atom force field for the purpose of phospholipid membrane simulations. The extension was done through reparametrization of torsional angle parameters. We tested the robustness of torsional parameters in the force field by changing the partial charges of the fragments of a DPPC molecule. To test the force field we performed molecular dynamics computer simulation on a system consisting of 64 DPPC phospholipid molecules and 1312 water molecules. Periodic boundary conditions were used to mimic the lamellar structure of the bilayers. The simulations were done at a constant pressure of 0 atm. The results that described the geometry of the bilayer and that included the area per head group, the repeat period, volume per lipid molecule, and a set of distances including the peak to peak distance in the electron density displayed a good agreement with the experiment. We showed that the area and volume per lipid depend on the parameters describing the hydrocarbon tails. The order parameter curve for the tails was also in good agreement with the experiment. The behavior of torsions in the head groups was also reason-

able and showed that it may deviate from that in the crystal and gel phases. More experimental information on head group configurations is desirable in order to make sure that the values of certain torsion angle parameters are correct. Likewise, our simulations display good agreement with previously published simulations of the DPPC/water system in the liquid crystal phase that used the CHARMM all atom force field. The advantage of using the united atom force field is in the reduction of computer time, and this can be very important for simulations of assemblies of biomolecules involving phospholipids. More detailed information on the order in the phospholipid membranes obtained from this simulation and a comparison with the most recent experimental data can be found elsewhere.[42]

Acknowledgments

We thank Dr. Lalith Perera and Dr. Ulrich Essmann for their assistance and comments. Calculations were performed on a Cray-T3E at the North Carolina Supercomputer Center and on a Cray-T3E at the San Diego Supercomputer Center. Computational support from NPACI is gratefully acknowledged.

References

1. Tobias, D. J.; Tu, K.; Klein, M. L. Curr Opin Colloid Interface Sci 1997, 2, 15.
2. Tu, K.; Tobias, D. J.; Klein, M. L. Biophys J 1995, 69, 2558.
3. Shinoda, W.; Namiki, N.; Okazaki, S. J Chem Phys 1994, 106, 5731.
4. Tieleman, D. P.; Berendsen, H. J. C. J Chem Phys 1996, 105, 4871.
5. Berger, O.; Edholm, O.; Jähnig, F. Biophys J 1997, 72, 2002.
6. Robinson, A. J.; Richards, W. G.; Thomas, P. J.; Hann, M. M. Biophys J 1994, 67, 2345.
7. Damodaran, K. V.; Merz, K. M. Langmuir 1994, 9, 1179.
8. Zhou, F.; Schulten, K. J Phys Chem 1995, 99, 2194.
9. Chiu, S.; Clark, M.; Balaji, V.; Subramaniam, S.; Scott, H.; Jacobsson, E. Biophys J 1995, 69, 1230.
10. Feller, S. E.; Zhang, Y.; Pastor, R. W. J Chem Phys 1995, 103, 10267.
11. Essmann, U.; Perera, L.; Berkowitz, M. L.; Darden, T.; Lee, H.; Pedersen, L. G. J Chem Phys 1995, 103, 8577.
12. Brooks, B. R.; Bruccoleri, R. E.; Olafson, B. D.; States, D. J.; Swaminathan, S.; Karplus, M. J Comput Chem 1983, 4, 187.
13. Feller, S. E.; Venable, R. M.; Pastor, R. W. Langmuir 1997, 13, 6555.
14. Woolf, T. B.; Roux, B. Proteins 1996, 24, 92.
15. Weiner, S. J.; Kollman, P. A.; Case, D. A.; Singh, U. C.; Ghio, C.; Alagonax, G.; Profeta, S.; Weiner, P. J Am Chem Soc 1984, 106, 765.
16. van Gunsteren, W. F.; Berendsen, H. J. C. Groningen Molecular Simulation (GROMOS) Library Manual; Biomos: Groningen, The Netherlands, 1987.
17. Schlenkrich, M.; Brickmann, J.; MacKerell, A. D., Jr.; Karplus, M. Biological Membranes; Birkhäuser: Berlin, 1996.
18. Pasenkiewicz−Gierula, M.; Takaoka, Y.; Miyagawa, H.; Kitamura, K.; Kusumi, A. J Phys Chem 1997, 101, 3677.
19. Jorgensen, W.; Tirado−Rives, J. J Am Chem Soc 1988, 110, 1657.
20. Ryckaert, J. P.; Bellemans, A. Chem Phys Lett 1975, 30, 123.
21. MacKerell, A. D., Jr.; Wiórkiewicz−Kuczera, J.; Karplus, M. J Am Chem Soc 1995, 117, 11946.
22. Cornell, W. D.; Cieplak, P.; Bayly, C. B.; Gould, I. R.; Mertz, K. M., Jr.; Ferguson, D. M.; Spellmeyer, D. S.; Fox, T.; Caldwell, J. W.; Kollman, P. A. J Am Chem Soc 1995, 117, 5179.
23. Stouch, T. R.; Ward, K. B.; Altieri, A.; Hagler, A. T. J Comput Chem 1991, 12, 1033.
24. Tu, K.; Tobias, D. J.; Klein, M. L. J Phys Chem 1995, 99, 10036.
25. Williams, G.; Owens, N. L.; Sheridan, J. Trans Faraday Soc 1971, 67, 922.
26. Vanderkooi, G. Biochemistry 1991, 30, 10760.
27. Jorgensen, W. L.; Chandrasekhar, J.; Madura, J. D.; Impey, R. W.; Klein, M. L. J Chem Phys 1983, 79, 926.
28. DL_POLY is a package of molecular simulation routines written by W. Smith and T. R. Forester, copyright The Council for the Central Laboratory of the Research Councils, Daresbury Laboratory at Daresbury, Nr. Warrington, UK, 1996.
29. Nagle, J. F.; Zhang, R. T.; Tristram−Nagle, S.; Sun, W. J.; Petrache, H. I.; Suter, R. M. Biophys J 1996, 70, 1419.
30. Nagle, J. F.; Weiner, M. C. Biochim Biophys Acta 1988, 942, 1.
31. Büldt, G.; Gally, H. U.; Sellig, J.; Zaccai, G. J Mol Biol 1979, 134, 673.
32. Egberts, E.; Berendsen, H. J. C. J Chem Phys 1988, 89, 3718.
33. Douliez, J. P.; Léonard, A.; Dufourc, E. J. Biophys J 1995, 68, 1727.
34. Mendelsohn, R.; Davies, M. A.; Chuster, H. F.; Xu, Z.; Bittman, R. Biochemistry 1991, 30, 8558.
35. Nagle, J. F.; Wilkinson, D. A. Biophys J 1978, 23, 159.
36. Gawrich, K.; Ruston, D.; Zimmerberg, J.; Parsegian, V.; Rand, R.; Fuller, N. Biophys J 1992, 61, 1213.
37. Essmann, U.; Perera, L.; Berkowitz, M. L. Langmuir 1995, 11, 4519.
38. Akitsu, R. H. Biochemistry 1981, 20, 7359.
39. Pearson, R. H.; Pasher, I. Nature 1979, 281, 499.
40. Tu, K.; Tobias, D. J.; Klein, M. L. Biophys J 1996, 70, 595.
41. Bicknell−Brown, E.; Brown, K. G.; Person, W. B. J Raman Spectrosc 1982, 12, 180.
42. Smondyrev, A. M.; Berkowitz, M. L. J Chem Phys to appear.
43. Hauser, H.; Pasher, I.; Pearson, R. H.; Sundell, S. Biochim Biophys Acta 1981, 650, 21.